Transportation Safety and Environment, 2022, **5**: tdac064

DOI: 10.1093/tse/tdac064
Advance access publication date: 21 December 2022
Research Article

Forecasting wind speed using a reinforcement learning hybrid ensemble model: a high-speed railways strong wind signal prediction study in Xinjiang, China

Bin Liu[1], Xinmin Pan[2], Rui Yang[3], Zhu Duan[3], Ye Li[3], Shi Yin[3], Nikolaos Nikitas[4] and Hui Liu[3,*]

[1]Research Institute of Science and Technology of China Railway Urumqi Group Co., Ltd., Urumqi 830011, Xinjiang, China;
[2]Xinjiang Uygur Autonomous Region Meteorological Service, Urumqi 830002, Xinjiang, China;
[3]School of Traffic and Transportation Engineering, Central South University, Changsha 410075, Hunan, China;
[4]School of Civil Engineering, University of Leeds, LS2 9JT, Leeds, UK.
*Corresponding author. E-mail: csuliuhui@csu.edu.cn

Abstract

Considering the application of wind-forecasting technology along the railway, it becomes an effective means to reduce the risk of train derailment and overturning. Accurate prediction of crosswinds can provide scientific guidance for safe train operation. To obtain more reliable wind-speed prediction results, this study proposes an intelligent ensemble forecasting method for strong winds along the high-speed railway. The method consists of three parts: the data preprocessing module, the hybrid prediction module and the reinforcement learning ensemble module. First, fast ensemble empirical model decomposition (FEEMD) is used to process the original wind speed data. Then, Broyden-Fletcher-Goldfarb-Shanno (BFGS) method, non-linear autoregressive network with exogenous inputs (NARX) and deep belief network (DBN), three benchmark predictors with different characteristics are employed to build prediction models for all the sublayers of decomposition. Finally, Q-learning is utilized to iteratively calculate the combined weights of the three models, and the prediction results of each sublayer are superimposed to obtain the model output. The real wind speed data of two railway stations in Xinjiang are used for experimental comparison. Experiments show that compared with the single benchmark model, the hybrid ensemble model has better accuracy and robustness for wind speed prediction along the railway. The 1-step forecasting results mean absolute error (MAE), mean absolute percentage error (MAPE) and root mean square error (RMSE) of Q-learning-FEEMD-BFGS-NARX-DBN in site #1 and site #2 are 0.0894 m/s, 0.6509%, 0.1146 m/s, and 0.0458 m/s, 0.2709%, 0.0616 m/s, respectively. The proposed ensemble model is a promising method for railway wind speed prediction.

Keywords: wind speed forecasting, high-speed railways, signal decomposition, reinforcement learning, ensemble model

1. Introduction

The emergence of the high-speed railway (HSR) system has connected different cities and accelerated the flow of talents and materials [1]. Convenient transportation makes the connection between cities closer, which greatly promotes the economic and cultural development of the areas along the railway line. The HSR technology has significant strategic significance [2]. However, the stability of high-speed trains during operation is easily affected by the environment, and the trains may overturn under the action of strong crosswinds [3]. In fact, train overturning incidents caused by strong crosswinds emerge in an endless stream, which seriously threatens the safety of railway transportation [4].

In response to train derailment accidents, scientists have studied the strong wind resistance performance of HSR. Sanquer et al. [5] designed an aerodynamic load measurement method based on pressure field and used it to evaluate the influence of aerodynamic force caused by crosswind on train operation stability. Cui et al. [6] calculated the safety domain conditions of the ultimate wind speed to ensure the safe operation of HSR by analysing the attitude changes of high-speed trains under the action of crosswind. Carrarini [7] used multi-body simulation modelling to analyse the risk of rolling stock overturning in cross-wind, and evaluated the influence of uncertainty parameters on stability. Cheli et al. [8] studied the relationship between cross-wind effect, aerodynamic load and HSR operation stability through aerodynamic numerical optimization experiments. Dorigatti et al. [9] developed a physical research model to compare the distribution of aerodynamic loads generated by transverse wind on HSR under static and dynamic conditions. Some aerodynamically optimized structures that can counteract the effects of high wind loads are explored.

Different from the above research ideas, some scientists have found that the railway strong wind warning system is a feasible means to effectively reduce train derailment accidents caused by crosswinds. Wind speed forecasts help train operators to implement more reliable speed limit warning instructions [10]. Early deceleration of trains can greatly reduce or even avoid rollovers [11]. To better manage the safety of train operations in the environment of large wind farms, research on wind speed prediction models has been carried out all over the world in recent years [12–14]. These systems measure the likelihood of overturning a train by comparing the predicted cross-wind strength with the

Received: June 17, 2022. **Revised:** October 19, 2022. **Accepted:** October 28, 2022

safety threshold. At present, wind speed prediction methods commonly used in railway systems include physical methods [15–18], statistical methods [19, 20] and artificial intelligence (AI) methods [12, 21, 22].

However, the existing prediction methods have certain limitations. First of all, the original wind signal collected by the anemometer has strong randomness, intermittency and volatility. If this kind of unstable noise is not preprocessed, it will bring great difficulties to the prediction work [23]. Second, the performance of a single AI model for wind speed prediction along railway lines cannot always be satisfactory. Due to the difference in adaptive characteristics, the model will show higher or lower prediction accuracy when faced with different application scenarios. The instability of its different ability to process data has brought difficulties to the forecasting work [24].

Aiming at the above technical bottlenecks, we propose a decomposition-prediction-ensemble framework in this study to improve the railway wind speed early warning systems. This model is designed to overcome the difficulty of volatility of original data and the unstable prediction performance of individual AI models. The main contributions of this paper can be summarized as follows:

1) The proposed reinforcement learning hybrid ensemble model combines the advantages of the fast ensemble empirical model decomposition (FEEMD) data pre-processing method and multiple basic predictors, and it can fully excavate the fluctuation information at different levels in the wind speed time series.

2) A preprocessing module for wind speed non-stationary series data is developed. The original non-stationary series processed by FEEMD has independent oscillatory components and is easier to predict. The randomness and volatility of wind speed data are effectively decomposed.

3) This study innovatively uses Q-learning to calculate the combined weights of Broyden-Fletcher-Goldfarb-Shanno (BFGS) algorithm, non-linear autoregressive network with exogenous inputs (NARX) and deep belief network (DBN), thereby realizing the organic ensemble of multiple sub-predictors, which avoids the limitations of a single model. The proposed Q-learning-FEEMD-BFGS-NARX-DBN (Q-FEEMD-BND) model integrates the characteristics of multiple models to show superior prediction accuracy in more scenarios.

The structure for the rest of this study is as follows. Section 2 introduces the methodology. Section 3 analyses and discusses the research area and the experimental case modelling results. Section 4 summarizes the research work and puts forward future prospects.

2. Methodology

2.1. Fast ensemble empirical model decomposition

As a variant of ensemble empirical mode decomposition (EEMD), the computation speed of FEEMD is improved and optimized [25]. In addition, FEEMD combines the idea of white noise and integrated mean, which cleverly solves the mode mixing problem of traditional algorithms, and it is suitable for solving non-stationary nonlinear series decomposition [26]. The specific implementation steps of FEEMD in this study are as follows:

1) Set the initial number of ensemble trials M.

2) Add a random Gaussian white noise signal $n_m(t)$ into the original unidirectional wind speed signal $x(t)$ to get the noise-enhanced signal $X_m(t)$.

$$X_m(t) = x(t) + n_m(t) \tag{1}$$

where, m is the number of iterations.

3) Implement standard EMD procedures. The noise signal $X_m(t)$ is decomposed into a series of intrinsic mode functions (IMFs) and a residual.

$$X_m(t) = \sum_{i=1}^{n} c_{i,m}(t) + o_{n,m}(t) \tag{2}$$

where, $c_{i,m}(t)$ is the i-th IMF of the m-th iteration, $o_{n,m}(t)$ is the residual of the m-th iteration and n is the total number of all IMFs.

4) Compare the magnitude of m and M. If $m < M$, update $m = m + 1$ and repeat steps (2) and (3). Different white noise sequences are added during each iteration of the loop.

5) Calculate the ensemble mean and residual for each IMF during M iterations.

$$c_i(t) = \frac{1}{M}\sum_{m=1}^{M} c_{i,m}(t),\ i = 1, 2, 3, ..., n,\ m = 1, 2, 3, ..., M \tag{3}$$

$$o_n(t) = \frac{1}{M}\sum_{m=1}^{M} o_{n,m}(t),\ m = 1, 2, 3, ..., M \tag{4}$$

where, $c_i(t)$ represents the i-th IMF component and $o_n(t)$ represents the final residual.

2.2 Broyden-Fletcher-Goldfarb-Shanno quasi-Newton back propagation

The BFGS is evolved from multilayer feedforward perceptron (MLP), and it is often used to solve the training optimization problem of the neural network [27]. The method has excellent convergence, and it is better than the back propagation neural network (BPNN) algorithm. The BFGS consists of input–hidden–output layers. Reasonable adjustment of the number of hidden layers and neuron parameters of the network can improve the nonlinear mapping ability. The BFGS network structure used in this study is presented in Fig. 1.

2.3 Non-linear autoregressive network with exogenous inputs

The NARX can overcome the influence of additional external input on the model, thereby ensuring the prediction accuracy of discrete-time series [28]. The NARX can simultaneously incorporate past states of the same series. Fig. 2 presents the model network of NARX.

The specific model output value can be expressed as follows:

$$y(k+1) = F\left[y(k), y(k-1), ..., y(k-d_o); X(k+1), X(k), ..., X(k-d_i)\right] \tag{5}$$

where, k is the number of neurons in the input layer, $y(k)$ represents the previous values of the target, $X(k)$ represents the exogenous associated series, and d_i and d_o represent the input and output lags. The output results of proper activation functions $f*(\cdot)$ with biases $b*$ can be given as follows [29]:

$$y(k+1) = f_o\left[\sum_{i=1}^{N_h} w_{oi}\cdot f_h\left(\sum_{i=0}^{d_i} w_{xi}X(k+1-i) + \sum_{i=0^{d_o}} w_{yi}y(k-i) + b_h\right) + b_o\right] \tag{6}$$

2.4 Deep belief network

The DBN is widely used in multiple fields, such as big data analysis, computer vision, text classification and so on [30]. Restricted

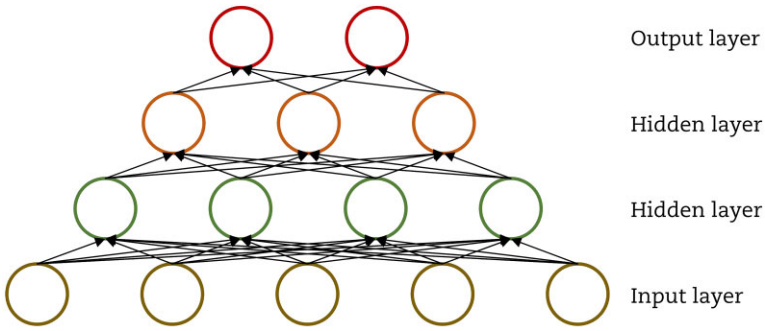

Fig. 1. The network structure of BFGS [31].

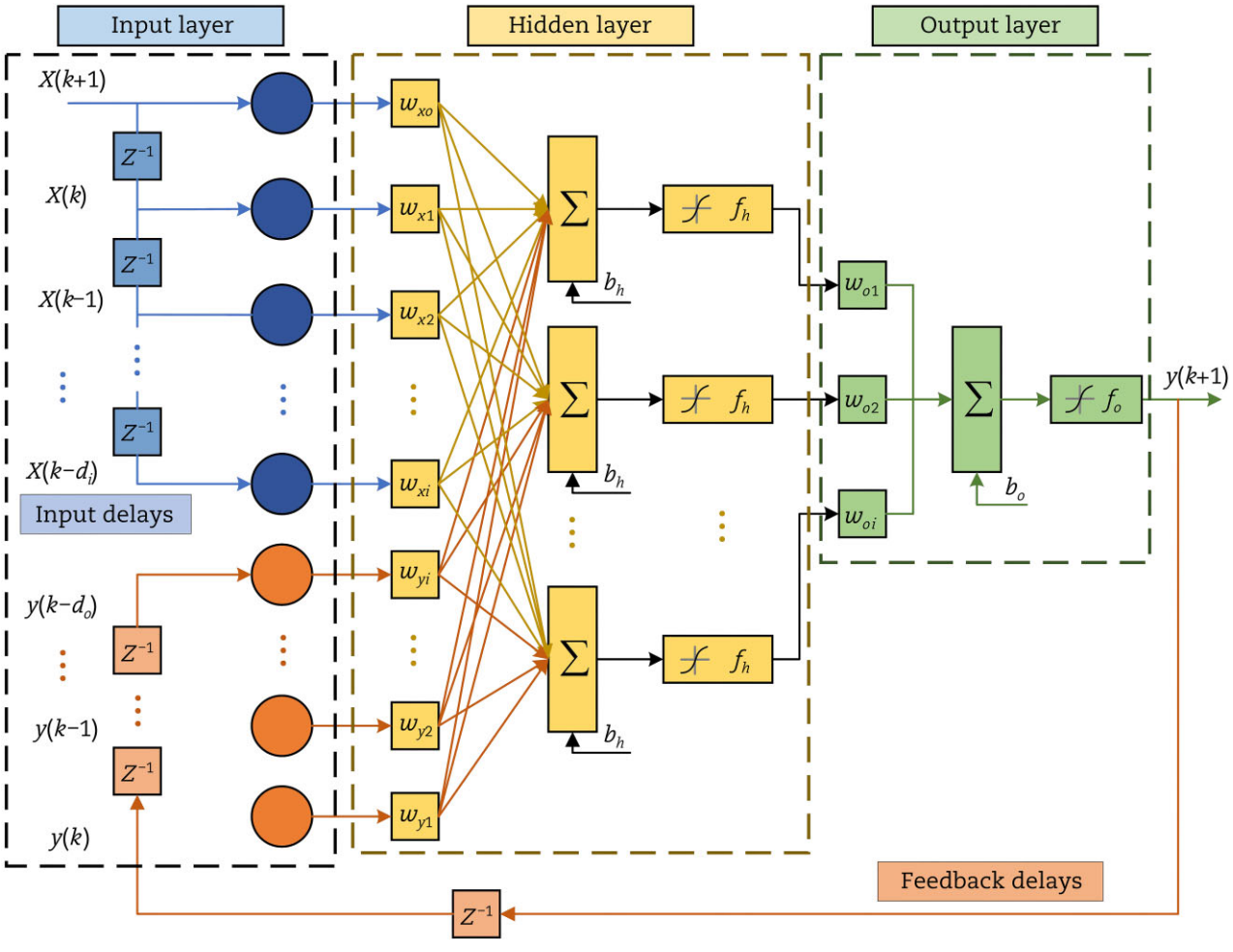

Fig. 2. The model architecture of NARX [32].

Boltzmann machines (RBMs) composed of multiple layers of random variables and latent variables are stacked in series to form a DBN, which enables top-down supervised learning. To avoid errors caused by human interference in the feature extraction process, the RBM intelligently converts the features in the original space into abstract representations in another space, layer by layer. Compared with the stacked autoencoder feature extraction method, DBN can obtain more information while generating less reconstruction error [33]. In this study, DBN is used for the task of deep learning prediction. Fig. 3 shows the principle of the DBN model.

2.5 Q-learning

Reinforcement learning emphasizes maximizing expected benefits through actions that change with the environment [34]. The reward and punishment mechanism can stimulate the agent to move towards the direction that produces the greatest benefit in the iterative process. As a typical efficient reinforcement learning method, Q-learning is used to solve the optimization problem of model fusion [24]. The Q reinforcement learning is used to combine multiple benchmark models through weighted integration. The organic integration of multiple benchmark predictors

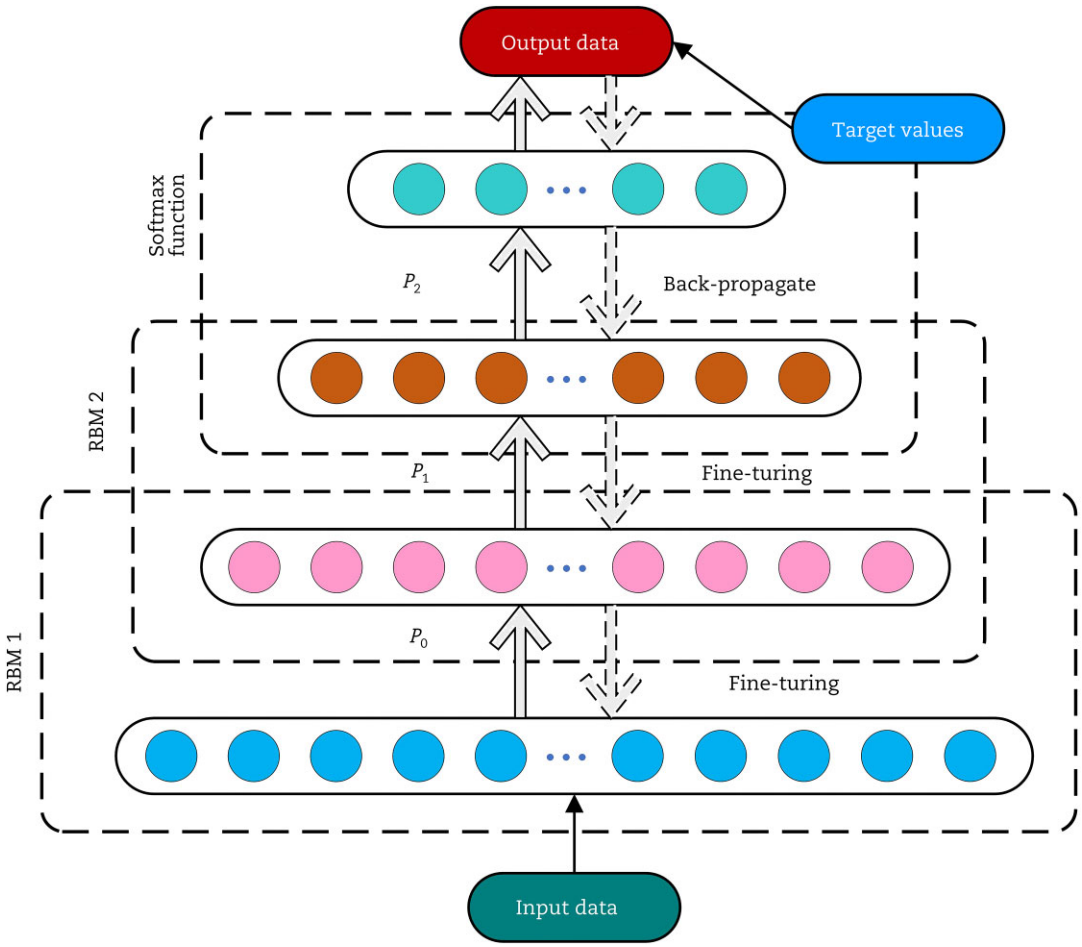

Fig. 3. The model framework of DBN [35].

can synthesize multiple advantages while alleviating the limitations of a single predictor. In this study, Q-learning is used for the weighted ensemble of BFGS, NARX and DBN.

To reasonably use the Q-learning algorithm, various parameters and states need to be initially set, including learning rates $\alpha(0 < \alpha < 1)$, work reward discounts $\gamma(0 < \gamma < 1)$, work greedy parameters ε, Q tables for ensemble learning, states $\boldsymbol{S} = \boldsymbol{S}_0$ and study strategies π. Take state $\boldsymbol{S}$ and action A as input to the Q agent to obtain the expectation of long-term payoff. The state $\boldsymbol{S} = [\omega_1, \omega_2, \omega_3]$ explains the composition of each specific state in the learning process, where $\omega_1, \omega_2, \omega_3$ represent the weight coefficients of BFGS, NARX and DBN.

$$\sum_{u=1}^{3} \omega_u = 1, \exists\ \omega_u \times \omega_u \geq 0 \tag{7}$$

Perform action $a_t = \pi^3(\boldsymbol{S}_t)$ based on the greedy strategy. After the environment is affected by the action, a new state and reward are returned to the agent.

$$a_t = \pi^3(\boldsymbol{S}_t) = \begin{cases} \text{Max}\,(Qvalue\ action), \in (1-\varepsilon) \\ \text{Randomly}\,(Qvalue\ action), \in \varepsilon \end{cases} \tag{8}$$

where, exploration probability $\varepsilon, 0 < \varepsilon < 1$.

By setting punishment and reward mechanisms for the Q agent to obtain rewards R and instant rewards r_t.

$$r_t = R(\boldsymbol{S}_t, a_t) \tag{9}$$

The reward and punishment mechanisms are set as follows:

$$R = \begin{cases} \Delta\text{error}(\boldsymbol{S}, \omega) - 1, & (\text{error}_{\text{old}} < \text{error}_{\text{new}}) \\ \Delta\text{error}(\boldsymbol{S}, \omega) + 1, & (\text{error}_{\text{old}} \geq \text{error}_{\text{new}}) \end{cases} \tag{10}$$
$$\Delta\text{error} = \text{error}_{\text{old}} - \text{error}_{\text{new}}$$

The prediction error MAPE (loss function) obtained from the weight coefficient and the old-new states is shown as follows:

$$\text{error}_{\text{MAPE}} = 1 \Big/ N_Y \sum_{i=1}^{N} \left(Y_i - \hat{Y}_i\right)^2 \tag{11}$$

where, $\hat{Y}$ represents the wind speed forecasting results, Y represents the real data and N_Y represents the amount of data.

The Q table and state $\boldsymbol{S}$ are updated according to the newly calculated evaluation function Q.

$$Q_{t+1}(\boldsymbol{S}_t, a_t) = Q_t(\boldsymbol{S}_t, a_t) + \alpha\left(r_t + \gamma \max_a Q_t(\boldsymbol{S}_{t+1}, a_{t+1}) - Q_t(\boldsymbol{S}_t, a_t)\right) \tag{12}$$

The above process is performed until the predicted target is reached or the number of iterations is terminated, and the final combined weights are obtained.

2.6 Framework of the proposed hybrid reinforcement learning model

Fig. 4 presents the details of the Q-learning integration process and the framework design of the proposed model (Q-FEEMD-BND). The model consists of three parts, which are the FEEMD data pre-

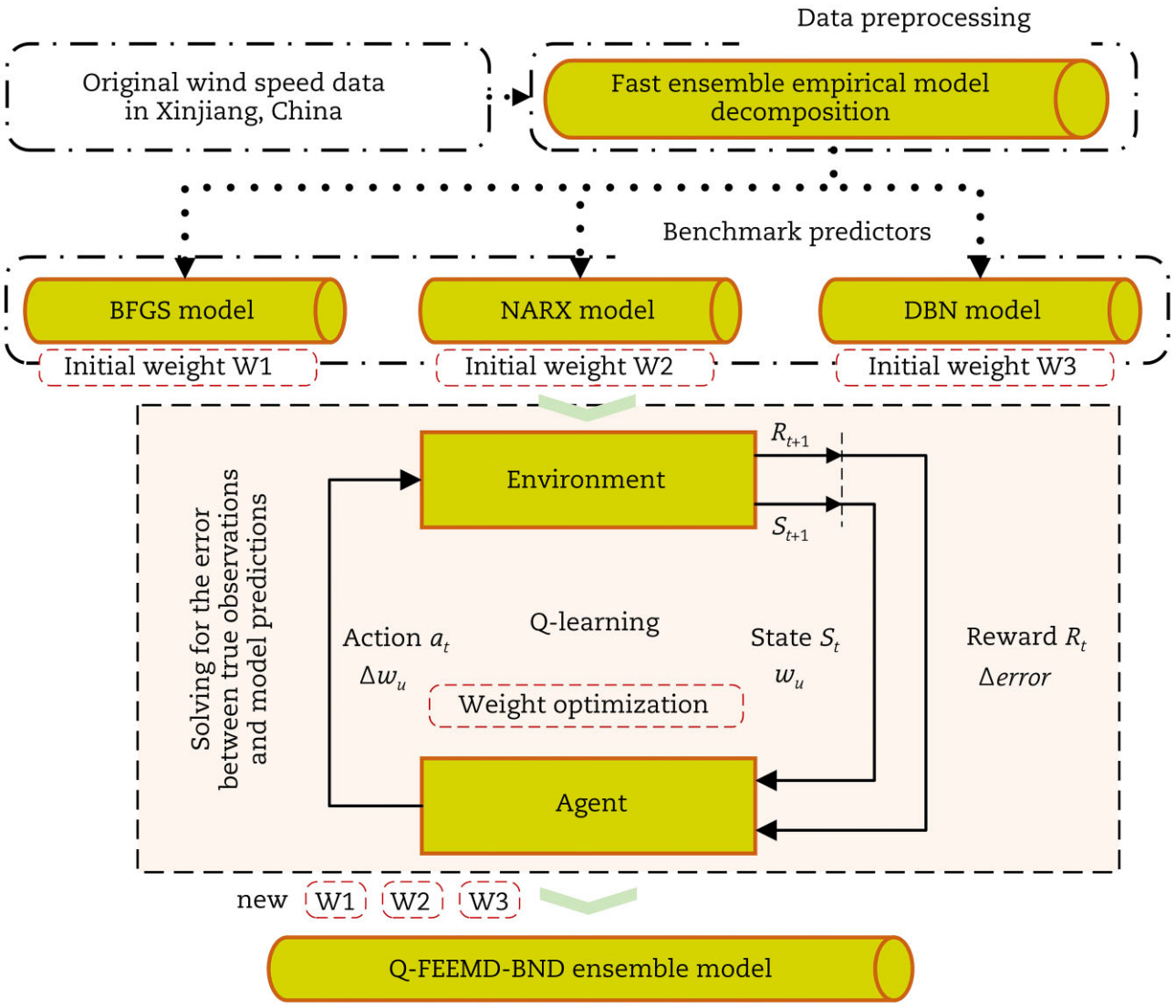

Fig. 4. The framework of strong wind signal prediction model along the HSR.

processing module, the hybrid prediction module and the reinforcement learning ensemble module.

2.6.1 *A module*

The original wind speed time series data are highly volatile, intermittent and unstable. To overcome the negative effects of such changes and build better prediction models, an improved decomposition method FEEMD is used to disassemble the oscillatory components of the dataset. This is to make the decomposed series easy to be learned by the predictor so as to obtain more accurate prediction results.

2.6.2 *B module*

The original wind speed data is sent to three predictors as input after the data pre-processing. As three benchmark predictors with different properties, BFGS, NARX and DBN can collect different wind speed change information. The benchmark predictor predicts each of the decomposed subseries and superimposes the subseries to obtain the final prediction result of the individual model.

2.6.3 *C module*

The Q-learning is utilized to optimize the weights of the above models iteratively. Finally, the new combined weights are used to organically integrate each benchmark model to obtain a reinforcement learning hybrid ensemble forecasting model.

3. Results and discussions

3.1 Study zones and data descriptions

The Xinjiang Province (China) is located in the Gobi desert, and its regional terrain is high in the north and low in the south. This caused the cold air from Siberia and the Ural Mountains to continue to strengthen during the downward moving process, resulting in strong and even super strong winds. The safety of train operations in a strong wind environment is greatly threatened. The wind speed data of the Baili wind area of the Xinjiang Lanxin Railway were used for experimental modelling, including total 6000 actual sampling data from two different wind measurement stations. Data from different sites verify the validity of the model. The sampling interval of wind speed signal points is 3 s. The 1st to 1200th sampling points of the original data are the training set,

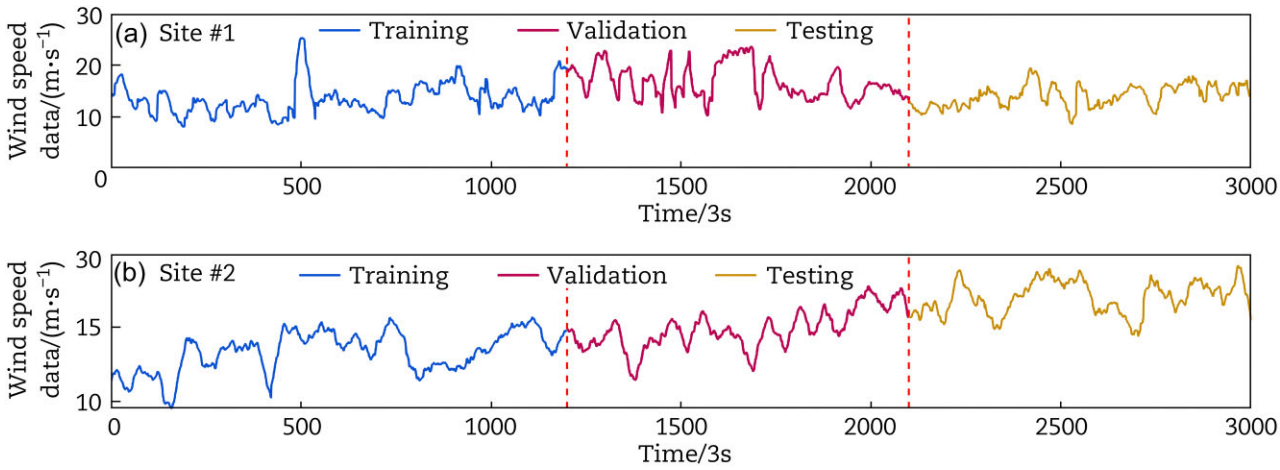

Fig. 5. The real wind speed dataset of (a) Site #1 and (b) Site #2.

Table 1. The wind speed forecasting results of each comparison model at Site #1.

Model	Horizon	Evaluation indicator		
		MAE (m/s)	MAPE (%)	RMSE (m/s)
BFGS	1-step	0.1996	1.4388	0.3571
	2-step	0.3680	2.6326	0.5741
	3-step	0.5206	3.7067	0.7587
NARX	1-step	0.2181	1.6252	0.4356
	2-step	0.4310	3.2959	1.1212
	3-step	0.5629	4.1386	0.8842
DBN	1-step	0.2027	1.4573	0.3530
	2-step	0.3716	2.6578	0.5653
	3-step	0.5229	3.7284	0.7439
FEEMD-BFGS	1-step	0.0932	0.6762	0.1214
	2-step	0.1305	0.9492	0.1787
	3-step	0.1919	1.4072	0.2435
FEEMD-NARX	1-step	0.0900	0.6552	0.1167
	2-step	0.1246	0.9065	0.1703
	3-step	0.1438	1.0587	0.2028
FEEMD-DBN	1-step	0.0980	0.7177	0.1261
	2-step	0.1234	0.9001	0.1848
	3-step	0.1482	1.0795	0.2166
Q-FEEMD-BND	1-step	0.0894	0.6509	0.1146
	2-step	0.1124	0.8187	0.1631
	3-step	0.1293	0.9498	0.1855

the 1201st to 2100th sampling points are the validation set and the 2101st to 3000th sampling points are the test set. Fig. 5 presents the specific fluctuations and partitioning of the data.

3.2 Performance evaluation indicators

To validate and evaluate the status of the reinforcement learning hybrid prediction model, three industry-accustomed error calculation metrics are used: mean absolute error (MAE), mean absolute percentage error (MAPE) and root mean square error (RMSE).

$$MAE = \left(\sum_{t=1}^{N_Y}\left|Y_t - \hat{Y}_t\right|\right) \Big/ N_Y \tag{13}$$

$$RMSE = \sqrt{\frac{1}{N_Y}\sum_{t=1}^{N_Y}\left(Y_t - \hat{Y}_t\right)^2} \tag{14}$$

$$MAPE = \left(\sum_{t=1}^{N_Y}\left|(Y_t - \hat{Y}_t)/Y_t\right|\right) \Big/ N_Y \tag{15}$$

where, $\hat{Y}$ is the forecasting results, Y is the real data and N_Y is the number of the real data.

3.3 Experimental study on prediction model

To demonstrate the strong wind warning performance, two actual Xinjiang wind speed forecasting datasets are used to design comparative experiments. First, BFGS, NARX and DBN predictors are constructed as three benchmark models. Then, FEEMD is used to perform data preprocessing. Finally, Q-learning is utilized to calculate the ensemble weights of the above three decomposition-prediction models to obtain the hybrid model. The comparative experiments can clearly reflect the independent performance of the models at each stage. The purpose of 1, 2 and 3 step prediction (3 s, 6 s and 9 s prediction) is to provide HSR system operators with more future wind speed prediction information to guide them to make reasonable judgement of wind avoidance in time. Tables 1 and 2 list the error indicators of the above seven mod-

Table 2. The wind speed forecasting results of each comparison model at Site #2.

Model	Horizon	Evaluation indicator		
		MAE (m/s)	MAPE (%)	RMSE (m/s)
BFGS	1-step	0.1559	0.8763	0.2554
	2-step	0.3245	1.8154	0.5441
	3-step	0.4990	2.7839	0.8346
NARX	1-step	0.1576	0.8871	0.2555
	2-step	0.2412	1.3687	0.3355
	3-step	0.3580	2.0223	0.5201
DBN	1-step	0.0799	0.4697	0.1075
	2-step	0.1322	0.7769	0.1732
	3-step	0.1814	1.0644	0.2373
FEEMD-BFGS	1-step	0.0496	0.2945	0.0664
	2-step	0.0785	0.4694	0.1086
	3-step	0.1394	0.8306	0.1811
FEEMD-NARX	1-step	0.0526	0.3089	0.0811
	2-step	0.0723	0.4217	0.2437
	3-step	0.0939	0.5470	0.2537
FEEMD-DBN	1-step	0.0487	0.2884	0.0620
	2-step	0.0569	0.3383	0.0734
	3-step	0.0651	0.3868	0.0848
Q-FEEMD-BND	1-step	0.0458	0.2709	0.0616
	2-step	0.0558	0.3317	0.0705
	3-step	0.0637	0.3780	0.0811

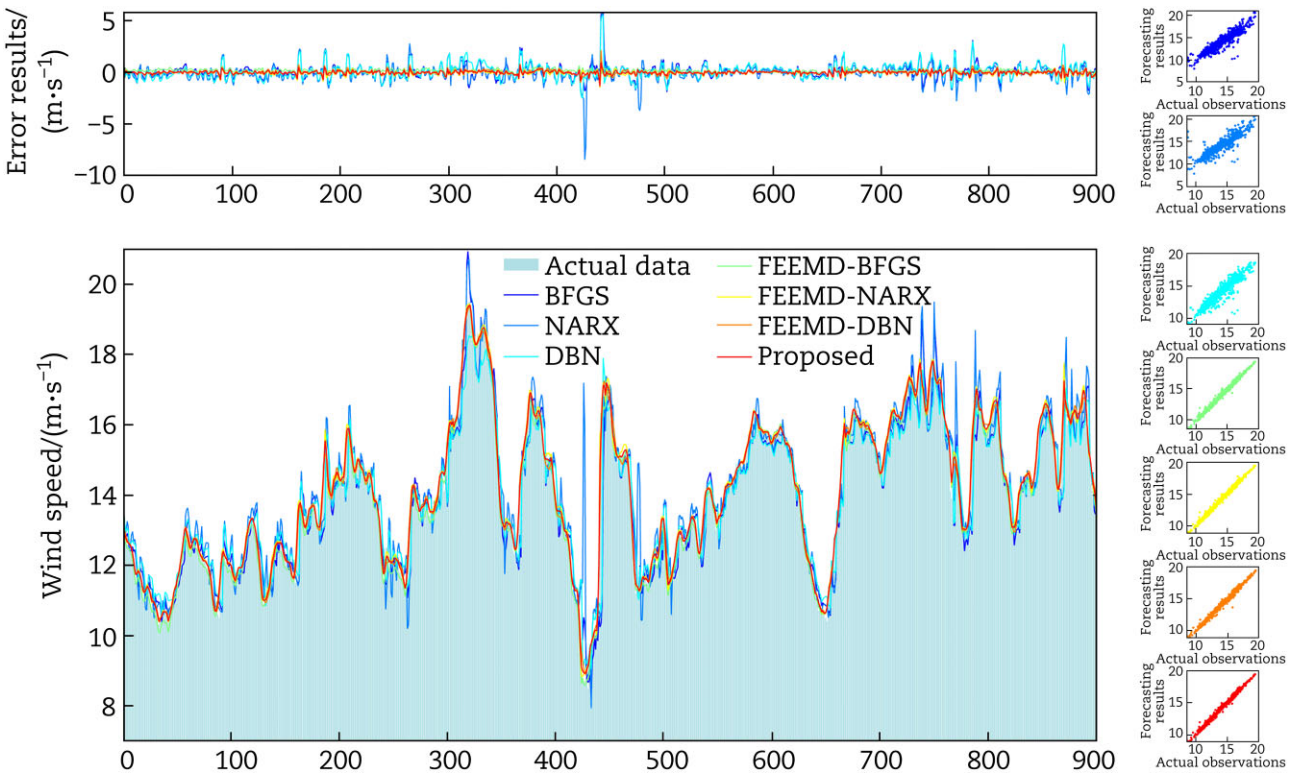

Fig. 6. The 3-step prediction performance of each model at Site #1.

els, including MAE, MAPE and RMSE. Figs. 6 and 7 show the fitting trend graph, scatter graph and error graph. The results and discussions are summarized as follows:

1) The BFGS, NARX and DBN do not accurately capture the future wind fluctuations very well. The experimental results show that the MAE, MAPE and RMSE of these three models are too large, which is not satisfactory. This may be due to the simple structure, poor adaptability and weak learning ability of a single base predictor. The wind speed series itself has strong uncertainty, volatility and instability. So the above benchmark model does not perform well.

2) The FEEMD can significantly improve the prediction accuracy of the benchmark models. The above three benchmark models can well track the change of wind speed time series after FEEMD

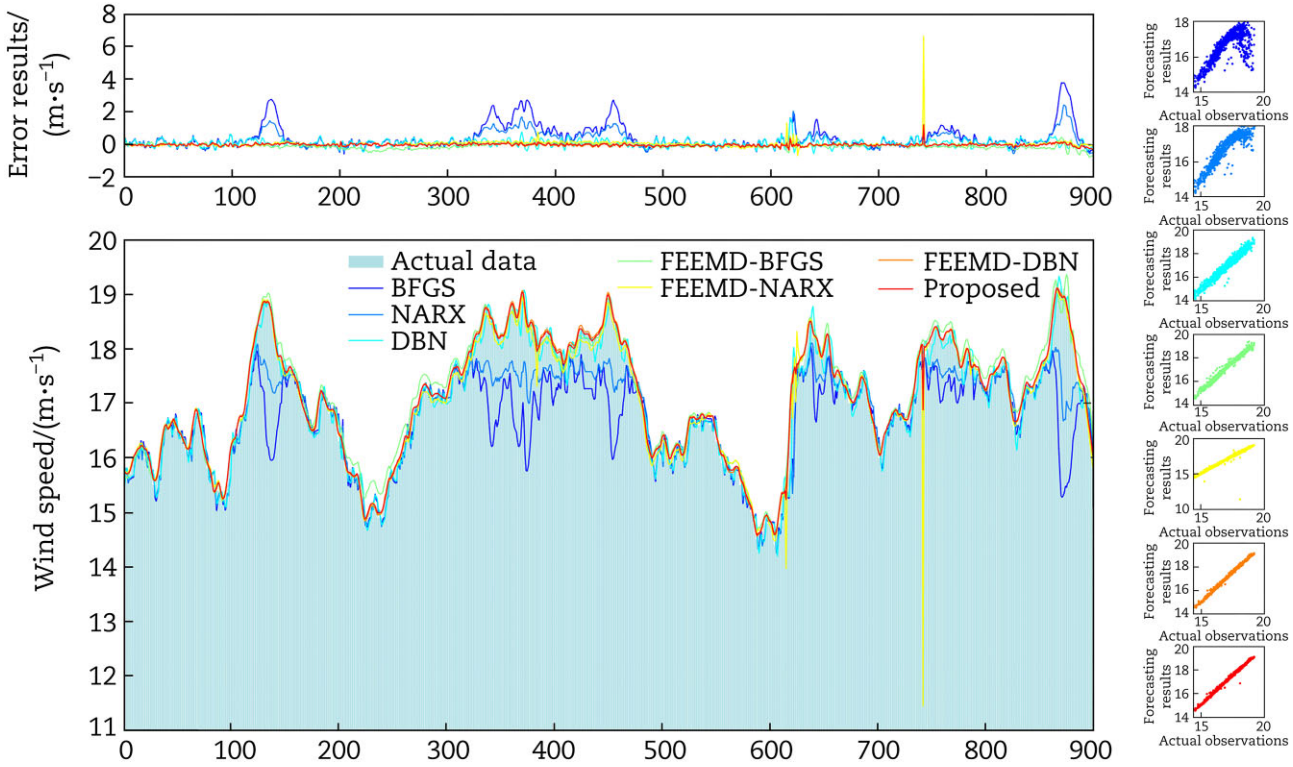

Fig. 7. The 3-step prediction performance of each model at Site #2.

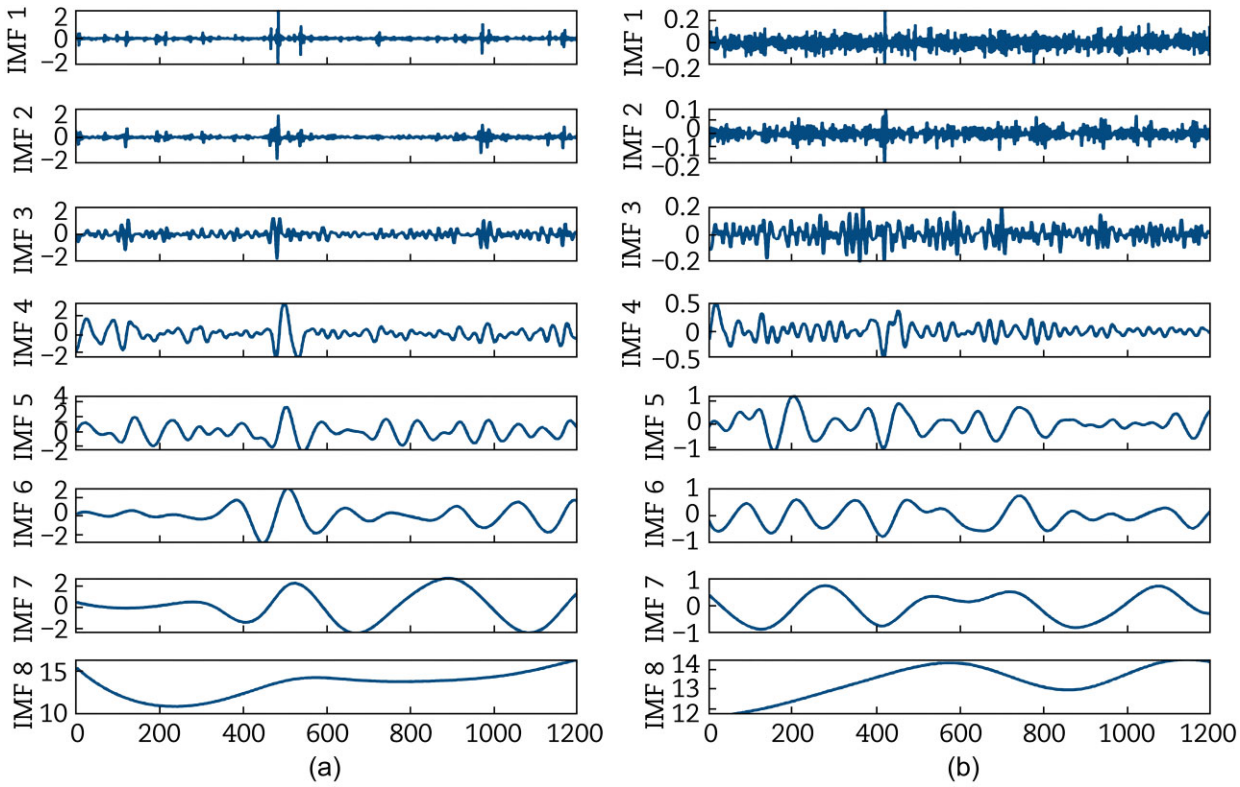

Fig. 8. The decomposition results of FEEMD in (a) Site #1, and (b) Site #2.

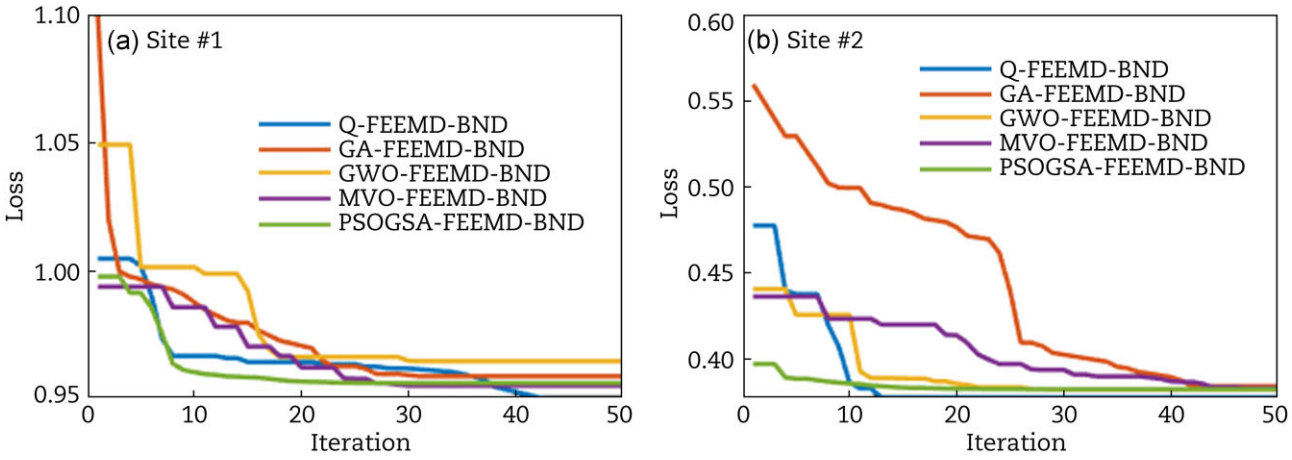

Fig. 9. Results of MAPE loss function during the iteration of Q-learning, GA, GWO, MVO and PSOGSA: (a) Site #1; (b) Site #2.

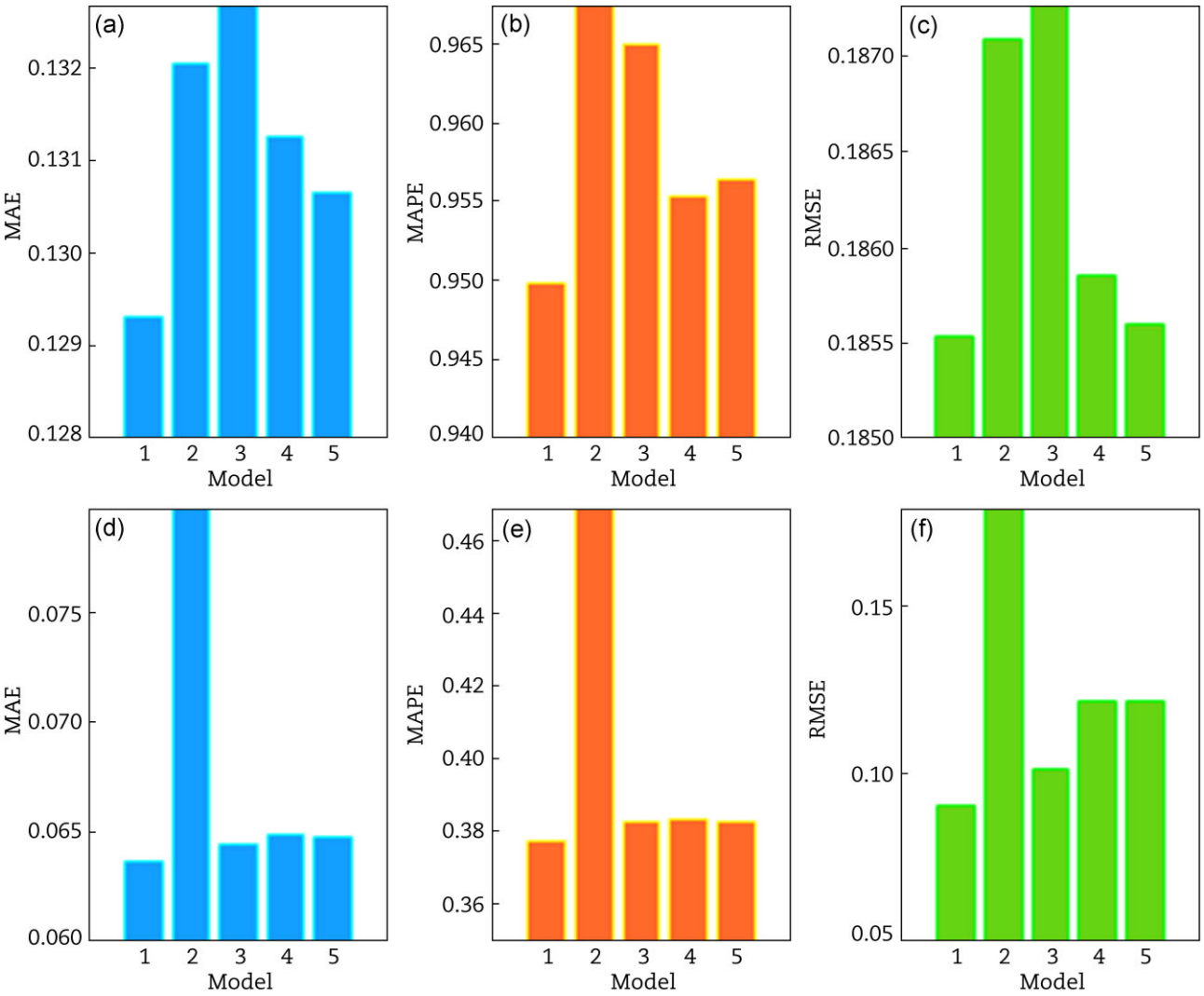

Fig. 10. The 3-step prediction error of Q-learning (Model 1), GA (Model 2), GWO (Model 3), MVO (Model 4) and PSOGSA (Model 5) ensemble methods: (a) MAE, Site #1; (b) MAPE, Site #1; (c) RMSE, Site #1; (d) MAE, Site #2; (e) MAPE, Site #2; (f) RMSE, Site #2.

Table 3. The computation time statistics of the proposed model.

Site	Time (s)		
	Training	Forecasting	Computation
1	59.77	0.56	60.33
2	63.89	0.73	64.62

decomposition preprocessing. This may be because FEEMD decomposes the original wind speed series into multiple highly stable subseries with independent oscillatory components. The decomposed subseries are easier to predict. In this experiment, the original series is decomposed into eight subseries with different oscillation amplitudes, as shown in Fig. 8. After that, benchmark predictors make the predictions for each subseries separately. The predictions are then superimposed to obtain the output of a single model, and the prediction results are shown in FEEMD-BFGS, FEEMD-NARX and FEEMD-DBN in Tables 1 and 2. This approach significantly reduces the prediction difficulty of the model.

3) The combined model after the Q-learning ensemble has the most satisfactory prediction accuracy. It is obvious that the prediction performance of several models is improved again after the ensemble operation. The reason for this phenomenon may be that reinforcement learning obtains the best model combination weights iteratively through a reasonable reward and punishment mechanism. The organic model combination effectively exerts the advantages of each benchmark model, thereby bursting out the maximum performance. In conclusion, the proposed hybrid model performs best in capturing the regularity of wind speed variation.

In addition, to prove the superiority of the Q-learning ensemble method, several meta-heuristic optimization algorithms are used to carry out ensemble experiment comparisons of the same group, including genetic algorithm (GA), grey wolf optimization (GWO), multi-verse optimization (MVO) and particle swarm optimization and gravitational search algorithm (PSOGSA). The prediction accuracy of the five different ensemble methods combined FEEMD-BFGS, FEEMD-NARX and FEEMD-DBN is verified by experiments. Fig. 9 illustrates the MAPE loss function of the ensemble model during 50 optimization iterations. Fig. 10 shows the prediction error of the combined model obtained by the above different ensemble algorithms.

As can be seen from the comparison and verification results in Figs. 9 and 10, the optimization ensemble effect of Q-learning is better than the other four comparison algorithms under the same number of iterations. The MAE, MAPE and RMSE of Q-FEEMD-BND are the smallest. This may be because the more scientific incentive and punishment mechanism of reinforcement learning makes the ensemble weights of the model iterate in a more scientific direction, so as to obtain a better weight combination.

4. Time property

It is necessary to consider constraints, such as computing time requirements and computing hardware limitations when building intelligent prediction models for wind along railway lines. In fact, ensuring the coherence and integrity of railway field forecasting is only meaningful when resources are limited. The modelling in this paper is carried out on a desktop computer with Windows 10, Intel(R) Core (TM) i7-9700 K CPU @ 3.60 GHz, 16.0 GB RAM and GTX 2070. Table 3 shows the model training time and prediction time under this operation condition. It can be found that the model training time of the two stations is 59.77 s and 63.89 s, respectively. In engineering applications, the point prediction results of 900 samples (about 2700 s) can be obtained by training such a model once, which can easily cover the modelling time cost and ensure the continuity of training. In addition, the prediction time is 0.56 s and 0.73 s respectively, which is significantly less than the time interval of data points (3 s). This result shows that the prediction process can predict the wind speed of 3 s in the future in a very short time. In general, the model proposed can perform the prediction work well under the computational constraints.

5. Conclusions and future works

The purpose of this paper is to design a cross-wind overturning risk prediction model for the HSR system to ensure the safety and stability of train operation. The framework of the intelligent wind prediction model along the railway is decomposition-prediction-ensemble. Comparative experiments show that the combination of the decomposition method and the multi-model ensemble module can make the predictor more robust and accurate. The FEEMD overcomes the difficulty of prediction caused by the unstable noise of the original wind speed signal. The ensemble method of Q-learning reinforcement learning integrates the model characteristics of BFGS, NARX and DBN by reasonable combination weights, which makes the data processing performance of the ensemble model better. The combined weight obtained by the Q ensemble method is better than that obtained by GA, GWO, MVO and PSOGSA. The accurate wind speed forecasting of the model can provide scientific guidance for the safety of railway transportation. Spatial correlation analysis methods of coupled spatiotemporal elements can be considered in future work. Information fusion of multiple sites in a region can avoid serious prediction errors caused by information distortion at a single site. In addition, the research on longer prediction steps and wind direction vectors also plays a very positive role in wind speed prediction.

Abbreviations

AI:	Artificial intelligence
BFGS:	Broyden-Fletcher-Goldfarb-Shanno
BPNN:	Back propagation neural network
DBN:	Deep belief network
EEMD:	Ensemble empirical mode decomposition
FEEMD:	Fast ensemble empirical model decomposition
GA:	Genetic algorithm
GWO:	Grey wolf optimization
HSR:	High-speed railway
IMFs:	Intrinsic mode functions
MAE:	Mean absolute error
MAPE:	Mean absolute percentage error
MLP:	Multilayer feedforward perceptron
MVO:	Multi-verse optimization
NARX:	Non-linear autoregressive network with exogenous inputs
PSOGSA:	Particle swarm optimization and gravitational search algorithm
Q-FEEMD-BND:	Q-learning-FEEMD-BFGS-NARX-DBN
RBM:	Restricted Boltzmann machine
RMSE:	Root mean square error

Acknowledgements

The study is fully supported by the Science and Technology Research and Development Program of China State Railway Group Co., Ltd. (Grant No. N2021T007), the National Natural Science Foundation of China (Grant No. 61873283) and the Changsha Science & Technology Project (Grant No. KQ1707017).

Conflict of interest statement

None declared.

References

1. Tian H. Review of research on high-speed railway aerodynamics in China. *Transportation Safety and Environment* 2019;**1**(1).
2. Lu C-f. A discussion on technologies for improving the operational speed of high-speed railway networks. *Transportation Safety and Environment* 2019;**1**:22–36.
3. Wang X, Qian Y, Chen Z et al. Numerical studies on aerodynamics of high-speed railway train subjected to strong crosswind. *Advances in Mechanical Engineering* 2019;**11**:1687814019887270.
4. Gou H, Chen X, Bao Y. A wind hazard warning system for safe and efficient operation of high-speed trains. *Automation in Construction* 2021;**132**:103952.
5. Sanquer S, Barre C, de Virel MD et al. Effect of cross winds on high-speed trains: development of a new experimental methodology. *Journal of Wind Engineering and Industrial Aerodynamics* 2004;**92**:535–45.
6. Cui T, Zhang W, Sun B. Investigation of train safety domain in cross wind in respect of attitude change. *Journal of Wind Engineering and Industrial Aerodynamics* 2014;**130**:75–87.
7. Carrarini A. Reliability based analysis of the crosswind stability of railway vehicles. *Journal of Wind Engineering and Industrial Aerodynamics* 2007;**95**:493–509.
8. Cheli F, Ripamonti F, Rocchi D et al. Aerodynamic behaviour investigation of the new EMUV250 train to cross wind. *Journal of Wind Engineering and Industrial Aerodynamics* 2010;**98**:189–201.
9. Dorigatti F, Sterling M, Baker C et al. Crosswind effects on the stability of a model passenger train—A comparison of static and moving experiments. *Journal of Wind Engineering and Industrial Aerodynamics* 2015;**138**:36–51.
10. Hoppmann U, Koenig S, Tielkes T et al. A short-term strong wind prediction model for railway application: design and verification. *Journal of Wind Engineering and Industrial Aerodynamics* 2002;**90**:1127–34.
11. Liu H, Liu C, He S et al. Short-term strong wind risk prediction for high-speed railway. *IEEE Transactions on Intelligent Transportation Systems* 2021;**22**:4243–55.
12. Yu C, Li Y, Xiang H et al. Data mining-assisted short-term wind speed forecasting by wavelet packet decomposition and Elman neural network. *Journal of Wind Engineering and Industrial Aerodynamics* 2018;**175**:136–43.
13. Liu H, Yang R, Wang T et al. A hybrid neural network model for short-term wind speed forecasting based on decomposition, multi-learner ensemble, and adaptive multiple error corrections. *Renewable Energy* 2021;**165**:573–94.
14. Liu H, Yang R, Duan Z. Wind speed forecasting using a new multi-factor fusion and multi-resolution ensemble model with real-time decomposition and adaptive error correction. *Energy Conversion and Management* 2020;**217**:112995.
15. Zhang Y, Li Y, Zhang G. Short-term wind power forecasting approach based on Seq2Seq model using NWP data. *Energy* 2020;**213**:118371.
16. Zhao J, Guo Z-H, Su Z-Y et al. An improved multi-step forecasting model based on WRF ensembles and creative fuzzy systems for wind speed. *Applied Energy* 2016;**162**:808–26.
17. Brabec M, Craciun A, Dumitrescu A. Hybrid numerical models for wind speed forecasting. *Journal of Atmospheric and Solar-Terrestrial Physics* 2021;**220**:105669.
18. Burlando M, Freda A, Ratto C et al. A pilot study of the wind speed along the Rome–Naples HS/HC railway line. Part 1—Numerical modelling and wind simulations. *Journal of Wind Engineering Industrial Aerodynamics* 2010;**98**:392–403.
19. Zhang H, Peng Z, Tang J et al. A multi-layer extreme learning machine refined by sparrow search algorithm and weighted mean filter for short-term multi-step wind speed forecasting. *Sustainable Energy Technologies and Assessments* 2022;**50**:101698.
20. Huang G, Liu R, Liu M et al. Modeling and simulating non-stationary thunderstorm winds based on multivariate AR-GARCH. *Journal of Wind Engineering and Industrial Aerodynamics* 2021;**211**:104565.
21. Zhang S, Wang C, Liao P et al. Wind speed forecasting based on model selection, fuzzy cluster, and multi-objective algorithm and wind energy simulation by Betz's theory. *Expert Systems with Applications* 2022;**193**:116509.
22. Nguyen THT, Phan QB. Hourly day ahead wind speed forecasting based on a hybrid model of EEMD, CNN-Bi-LSTM embedded with GA optimization. *Energy Reports* 2022;**8**:53–60.
23. Liu H, Tian H-q, Li Y-f. An EMD-recursive ARIMA method to predict wind speed for railway strong wind warning system. *Journal of Wind Engineering and Industrial Aerodynamics* 2015;**141**:27–38.
24. Yang R, Liu H, Nikitas N et al. Short-term wind speed forecasting using deep reinforcement learning with improved multiple error correction approach. *Energy* 2022;**239**:122128.
25. Wang Y-H, Yeh C-H, Young H-WV et al. On the computational complexity of the empirical mode decomposition algorithm. *Physica A: Statistical Mechanics and its Applications* 2014;**400**:159–67.
26. Wu Z, Huang NE. Ensemble empirical mode decomposition: a noise-assisted data analysis method. *Advances in adaptive data analysis* 2009;**1**:1–41.
27. Anam S. Rainfall prediction using backpropagation algorithm optimized by Broyden-Fletcher-Goldfarb-Shanno algorithm. in *IOP Conference Series: Materials Science and Engineering*, 2019, vol. **567**, p. 012008: IOP Publishing.
28. Huang J-h, Liu H. A hybrid decomposition-boosting model for short-term multi-step solar radiation forecasting with NARX neural network. *Journal of Central South University* 2021;**28**:507–26.
29. Zhao M, Zhang R, Lin C et al. Stochastic model predictive control for dual-motor battery electric bus based on signed Markov chain Monte Carlo method. *IEEE Access* 2020;**8**:120785–97.
30. Zhang P, Ci B. Deep belief network for gold price forecasting. *Resources Policy* 2020;**69**:101806.
31. Nawi NM, Ransing MR, Ransing RS. An improved learning algorithm based on the Broyden-Fletcher-Goldfarb-Shanno (BFGS) method for back propagation neural networks. in *Sixth International Conference on Intelligent Systems Design and Applications*, 2006, vol. **1**, pp. 152–7: IEEE.
32. Erwinski K, Paprocki M, Wawrzak A et al. Neural network contour error predictor in CNC control systems. in *2016 21st Interna-*

tional Conference on Methods and Models in Automation and Robotics (MMAR), 2016, pp. 537–42: IEEE.

33. Khodayar M, Saffari M, Williams M et al. Interval deep learning architecture with rough pattern recognition and fuzzy inference for short-term wind speed forecasting. *Energy* 2022;**254**:124143.
34. Kaelbling LP, Littman ML, Moore AW. Reinforcement learning: a survey. *Journal of Artificial Intelligence Research* 1996;**4**:237–85.
35. Hu S, Xiang Y, Huo D et al. An improved deep belief network based hybrid forecasting method for wind power. *Energy* 2021;**224**:120185.

Received: June 17, 2022. **Revised:** October 19, 2022. **Accepted:** October 28, 2022